

1 **Metrics for linking emissions of gases and aerosols to global precipitation changes**

2 K. P. Shine^{1,*}, R. P. Allan¹, W. J. Collins¹ and J. S. Fuglestedt³

3 ¹Department of Meteorology, University of Reading, UK

4 ²CICERO - Center for International Climate and Environmental Research–Oslo, Oslo,
5 Norway

6 *Corresponding author – email: k.p.shine@reading.ac.uk

7

8 **Abstract**

9 Recent advances in understanding have made it possible to relate global precipitation changes
10 directly to emissions of particular gases and aerosols that influence climate. Using these
11 advances, new indices are developed here called the Global Precipitation-change Potential for
12 pulse (GPP_P) and sustained (GPP_S) emissions, which measure the precipitation change per
13 unit mass of emissions.

14 The GPP can be used as a metric to compare the effects of different emissions. This is akin to
15 the global warming potential (GWP) and the global temperature-change potential (GTP)
16 which are used to place emissions on a common scale. Hence the GPP provides an additional
17 perspective of the relative or absolute effects of emissions. It is however recognised that
18 precipitation changes are predicted to be highly variable in size and sign between different
19 regions and this limits the usefulness of a purely global metric.

20 The GPP_P and GPP_S formulation consists of two terms, one dependent on the surface
21 temperature change and the other dependent on the atmospheric component of the radiative
22 forcing. For some forcing agents, and notably for CO_2 , these two terms oppose each other –
23 as the forcing and temperature perturbations have different timescales, even the sign of the
24 absolute GPP_P and GPP_S varies with time, and the opposing terms can make values sensitive
25 to uncertainties in input parameters. This makes the choice of CO_2 as a reference gas
26 problematic, especially for the GPP_S at time horizons less than about 60 years. In addition,
27 few studies have presented results for the surface/atmosphere partitioning of different
28 forcings, leading to more uncertainty in quantifying the GPP than the GWP or GTP.

29 Values of the GPP_P and GPP_S for five long- and short-lived forcing agents (CO_2 , CH_4 , N_2O ,
30 sulphate and black carbon (BC)) are presented, using illustrative values of required
31 parameters. The resulting precipitation changes are given as the change at a specific time
32 horizon (and hence they are end-point metrics) but it is noted that the GPP_S can also be
33 interpreted as the time-integrated effect of a pulse emission. Using CO_2 as a reference gas,
34 the GPP_P and GPP_S for the non- CO_2 species are larger than the corresponding GTP values.
35 For BC emissions, the atmospheric forcing is sufficiently strong that the GPP_S is opposite in
36 sign to the GTP_S . The sensitivity of these values to a number of input parameters is explored.

37 The GPP can also be used to evaluate the contribution of different emissions to precipitation
38 change during or after a period of emissions. As an illustration, the precipitation changes
39 resulting from emissions in 2008 (using the GPP_P) and emissions sustained at 2008 levels
40 (using the GPP_S) are presented. These indicate that for periods of 20 years (after the 2008
41 emissions) and 50 years (for sustained emissions at 2008 levels) methane is the dominant
42 driver of positive precipitation changes due to those emissions. For sustained emissions, the
43 sum of the effect of the 5 species included here does not become positive until after 50 years,
44 by which time the global surface temperature increase exceeds 1 K.

45

46 **1. Introduction**

47 A broad range of emissions of gases and aerosols influence climate, either directly or
48 indirectly. That influence depends on the characteristics of the gases and aerosols, such as
49 their lifetime, and their ability to influence the radiation budget. The conventional cause-and-
50 effect chain links emissions to changes in concentrations, which then cause a radiative
51 forcing with subsequent downstream effects on, for example, temperature, precipitation and
52 sea level. By exploiting understanding of the characteristics of the gases and aerosols, in
53 concert with simplified descriptions of the climate system, it is possible to develop simple
54 methodologies that relate emissions directly to climate impacts, rather than having to
55 explicitly account for the intermediate steps. Such methodologies have pedagogic value in
56 making clearer the link between emissions (rather than, for example, concentration changes)
57 and climate response and they also have potential applications. The purpose of this paper is to
58 present a methodology that links global-mean precipitation directly to emissions of different
59 gases and aerosols. This exploits recent advances in understanding of how radiative forcing
60 (RF) and temperature change influence precipitation change. The methodology presented
61 here yields what we call the Global Precipitation-change Potential (GPP), which is the global-
62 mean precipitation change per unit mass of emission. The GPP is presented for both pulse
63 and sustained emissions.

64 The impact of climate change depends on more than just global temperature change. Hence
65 the development of a methodology linking emissions directly to precipitation is attractive.
66 However, projections from ensembles of climate model simulations show that precipitation
67 change is much less amenable to a global representation than temperature change. The
68 projections indicate that the average surface temperature response to increased concentrations
69 of greenhouse gases later in this century is largely the same sign over the whole planet, the
70 temperature changes are coherent on large spatial scales, and climate models largely agree on
71 the pattern of temperature change, if not the absolute size (e.g. Knutti and Sendlāček 2012).
72 By contrast, projected precipitation changes vary regionally in sign, are spatially much more
73 variable and there is much less agreement between climate models on the patterns of response
74 (e.g. Knutti and Sendlāček 2012). One part of the spatial pattern of precipitation change can
75 be understood in quite simple terms, as being due to the enhanced convergence and
76 divergence of moisture in a warmer and moister atmosphere, assuming no change in the
77 atmospheric flow that transports the moisture (Held and Soden 2006). Other parts stem from
78 changes in atmospheric circulation and surface water availability in response to forcing, and
79 from internal variability; the response and variability differ between climate models, leading
80 to the diverse model projections of precipitation change. Nevertheless, the global-mean
81 precipitation response is coherent amongst these climate models such that over the 21st
82 century, precipitation is projected to increase by about 1 to 3% per degree C of global-mean
83 warming (e.g. Collins et al. 2013). This paper addresses the dependence of this global-mean
84 component of precipitation change on the emitted species, as global-mean precipitation
85 changes can be taken as being a useful indicator of the size of disturbance of the global
86 hydrological cycle.

87 Section 2 presents a brief overview of emission metrics which are used to place emissions of
88 different gases on some common (usually CO₂-equivalent) scale, as this is one potential
89 application of the GPP. Section 3 presents the simple conceptual model that is used to relate
90 precipitation change to RF and temperature change, which are themselves related to
91 emissions. Section 4 presents some illustrative examples of the GPP drawing values of key
92 parameters from the literature. Section 5 then uses the methodology in the context of climate
93 metrics, and compares it with more conventional metrics (the Global Warming Potential
94 (GWP) and Global Temperature-change Potential (GTP)). Section 6 presents an illustration
95 of the use of the methodology for understanding the effects of emissions in an individual year
96 (or sustained emissions from that year) on precipitation changes in or after that year – this
97 illustrates the principal drivers of the precipitation change, given present-day emissions.
98 Section 7 explores some aspects of the uncertainty in characterising the GPP and Section 8
99 discusses prospects for further developing the GPP, including possibilities for including more
100 regional-scale information on precipitation response.

101 It is noted that Shindell et al. (2012) have demonstrated a link between radiative forcing (due
102 to a variety of forcing mechanisms) in specific latitude bands to precipitation change in a
103 number of selected regions; their precipitation change per unit radiative forcing was called a
104 “Regional Precipitation Potential”, which is distinct from the GPP framework presented here,
105 where the precipitation change is directly related to emissions.

106 **2. The utility of emission metrics**

107 One potential application of the GPP is to place emissions of different species on a common
108 scale, in a similar way to the GWP. The 100-year time-horizon GWP (GWP(100)) is used by
109 the Kyoto Protocol to the United Nations’ Framework Convention on Climate Change to
110 place emissions of many relatively well-mixed non-CO₂ greenhouse gases on a so-called
111 “CO₂-equivalent scale”; this is necessary for the type of multi-gas treaty that the Kyoto
112 Protocol represents. Metrics such as the GWP can also be used in life-cycle assessment and
113 carbon footprint studies, for assessing possible mitigation strategies, for example in particular
114 economic sectors, and can extend beyond the gases included in the Kyoto Protocol (see e.g.,
115 Fuglestvedt et al. 2010, Deuber et al. 2014).

116 The GWP characterises the RF in response to a pulse emission of a substance, integrated over
117 some specified time horizon. It is normally expressed relative to the same quantity for an
118 equal-mass emission of CO₂. The GWP has enabled the multi-gas operation of the Kyoto
119 Protocol but has also been the subject of criticism for some applications (e.g., Myhre et al.
120 (2013), Pierrehumbert (2014) and references therein). This is partly because the use of time-
121 integrated RF does not unambiguously relate to an impact of climate change (such as
122 temperature change) and also because it contains value judgements (particularly the choice of
123 time horizon) that cannot be rigorously justified for any particular application (Myhre et al.,
124 2013).

125 Metrics that extend beyond time-integrated forcing have also been proposed. The GTP (e.g.,
126 Shine et al. 2007; Myhre et al. 2013) characterises the global-mean surface temperature

127 change at some time after an emission. It may be more applicable to policies that aim to
128 restrict temperature change below a given target level. The GTP is also subject to criticism
129 and the need for value judgements when choosing time horizons (Myhre et al. 2013).
130 Nevertheless the GTP (and its variants, such as the mean global temperature-change potential
131 (e.g., Gillett and Matthews 2010, Deuber et al. 2014) and integrated temperature potential
132 (e.g., Peters et al. 2011, Azar and Johansson, 2012)) do at least extend to a parameter
133 (temperature change) more obviously related to a climate change impact. Sterner et al. (2014)
134 recently presented a metric for sea-level rise. Metrics can also be derived numerically on the
135 basis of the contribution of an emission of a component at a given time, to temperature
136 change (or other parameters) during some future period, as simulated by a simple climate
137 model driven by a specific emissions scenario (e.g. Tanaka et al. 2009).

138 Metrics can also be extended to the economic effects of an emission (for example the Global
139 Cost Potential and Global Damage Potential), by relating the metrics to costs and damages
140 (e.g., Johansson 2012) and in certain restrictive cases these can be shown to have equivalence
141 to physically-based metrics such as the GWP and GTP (e.g., Tol et al. 2012). One difficulty
142 in such approaches is that the economic damage has to be represented in a highly-idealised
143 form, as some simple function of, for example, global-mean temperature change.
144 Conventional physical metrics can also be judged in an economic context (e.g., Reisinger et
145 al. 2013, Strefler et al. 2014).

146 The GPP enables an additional and complementary methodology to existing methods for
147 intercomparing the impacts of emissions of difference species, and the impact of actual or
148 proposed changes in those emissions.

149 **3. Simple conceptual model**

150 **3.1 Relationships between radiative forcing and changes in temperature and** 151 **precipitation**

152 The simple conceptual model presented here originates from the analysis of simulated
153 precipitation changes in response to increases in CO₂ presented by Mitchell et al. (1987). This
154 analysis was based around the fundamental controls on the energy balance of the troposphere,
155 in which, to first order, the latent heating resulting from the net rate of condensation of water
156 vapour (and hence precipitation) is balanced by net radiative cooling. The conceptual model
157 has been further developed more recently, and extended to both multi-model assessments and
158 other climate forcing (and feedback) mechanisms (e.g., Allen and Ingram, 2002, Takahashi
159 2009, Andrews et al. 2010, Kvalevåg et al. 2013, Allan et al. 2014).

160 The framework starts with an expression of the global-mean atmospheric energy budget,
161 whereby the net emission of radiation by the atmosphere (i.e. the atmospheric radiative
162 divergence (R_d), which is the sum of the emission of longwave radiation by the atmosphere
163 minus the atmospheric absorption of longwave and shortwave radiation) is balanced by the
164 input of surface sensible (SH) and latent (LH) heat fluxes so that

$$165 \quad R_d = LH + SH. \quad (1)$$

166 LH is directly related to the precipitation as, at the global-mean level, evaporation (and hence
 167 LH fluxes) and precipitation approximately balance.

168 In response to the imposition of an RF and subsequent changes in temperature, humidity and
 169 clouds, R_d will change. The latent heat change ΔLH can then be written

$$170 \quad \Delta LH = \Delta R_d - \Delta SH. \quad (2)$$

171 ΔLH in W m^{-2} can be converted to precipitation units of mm day^{-1} by multiplication by 0.034
 172 (86400 seconds in a day divided by the latent heat of vaporisation, L ($2.5 \times 10^6 \text{ J kg}^{-1}$ at
 173 273.15 K)). There is some level of approximation in this conversion, as L is temperature
 174 dependent and some precipitation falls as snow rather than rain, and hence the latent heat of
 175 sublimation would be more appropriate. The precipitation change could also be quoted in %
 176 of global-mean precipitation (about 2.68 mm day^{-1} (e.g., Huffman et al., 2009)).

177 ΔR_d has two components. The first component is due directly to the RF mechanism which can
 178 change the absorption of shortwave radiation and/or the emission and absorption of longwave
 179 radiation. The conventional top-of-atmosphere radiative forcing (RF) can be written as the
 180 sum of a surface component (RF_s) and an atmospheric component (RF_a), and it is RF_a that
 181 directly influences ΔR_d . Because values of RF are more readily available than RF_a for a wide
 182 range of constituents, it is convenient to relate RF_a to RF and so, following Allan et al.
 183 (2014), we define a parameter f such that $RF_a = f RF$. The parameter f could be estimated
 184 directly from RF calculations using a radiative transfer code. However, here results from
 185 fixed-sea-surface-temperature climate model simulations (e.g. Andrews et al. 2010, Kvalevåg
 186 et al. 2013) are used; these have the advantage that they include the impact on f of rapid
 187 adjustments of, for example, clouds. A disadvantage is that the results of such experiments
 188 are noisier, because of model internal variability, which can be particularly important for
 189 small forcings. Note that a fully consistent approach would adopt effective radiative forcings
 190 (ERF – see Myhre et al. (2013)) rather than RF, and values of f derived using ERFs.
 191 However, assessed values of ERFs are not available for many species and so, in common
 192 with Myhre et al., (2013), the metric values calculated here use RFs, but include a number of
 193 indirect chemical effects and some cloud effects, as noted in Section 4. The values of f are
 194 based on one method of deriving ERFs and a possible reason for differences between f values
 195 in Andrews et al. (2010) and Kvalevåg et al. (2013) (see Section 7) is that the fast
 196 tropospheric responses that distinguish RF from ERF differ between the models used in their
 197 studies.

198 The second component of ΔR_d is due to the temperature change resulting from the RF, which
 199 leads to changes in emission of longwave radiation. This change is modified by feedbacks
 200 involving other radiatively-important components such as water vapour and clouds (e.g.
 201 Takahashi, 2009, Previdi 2010) which can also influence ΔR_d via the absorption of shortwave
 202 radiation. Climate model simulations indicate that this component of ΔR_d varies
 203 approximately linearly with changes in global-mean surface temperature ΔT_s (e.g., Lambert
 204 and Webb, 2008, Previdi 2010, O’Gorman et al. 2012).

205 ΔSH in Eq. (2) is less well constrained. It also has two components, one due to the fast
 206 response to RF, which is independent of surface temperature change, and one due to surface
 207 temperature change. The fast response has been shown to be small for greenhouse gas
 208 forcings; Andrews et al. (2010) and Kvalevåg et al. (2013) show it to be typically less than
 209 10% of ΔLH for a doubling of CO_2 , although the size and sign varies can vary amongst
 210 models (Andrews et al. (2009)). However, it can be much larger for other forcings (of order
 211 50% of ΔLH in the case of black carbon (Andrews et al. (2010) and Kvalevåg et al (2013))). As
 212 noted by Takahashi (2009) and O’Gorman et al. (2012) an improved conceptual model could
 213 distinguish between ΔR_d for the whole atmosphere and ΔR_d for the atmosphere above the
 214 surface boundary layer; changes in ΔR_d within the boundary layer seem more effective at
 215 changing SH (e.g. Ming et al. (2010)) and hence less effective at changing LH. Here,
 216 following Thorpe and Andrews (2014), we assume the fast component ΔSH to be small and
 217 neglect it, but more work in this area is clearly needed.

218 Lambert and Webb (2008), Previdi (2010), O’Gorman et al. (2012) and others show that
 219 while generally a smaller term, the surface temperature dependent part of ΔSH has a similar
 220 dependency on ΔT_s (at least in the multi-model mean) as ΔR_d . Hence it is convenient to
 221 combine the ΔT_s -related changes in R_d and this component of SH in Eq. (2) into a single term
 222 dependent on ΔT_s and separate out the RF term. Equation (2) then becomes, in precipitation
 223 units of $mm\ day^{-1}$,

$$224 \quad \Delta P = 0.034(k\Delta T_s - fRF). \quad (3)$$

225 Despite its apparent simplicity, Eq. (3) has been shown by Thorpe and Andrews (2014) to
 226 reasonably well simulate future projections of global-mean precipitation change from a range
 227 of atmosphere-ocean general circulation models, albeit with a tendency to underestimate the
 228 multi-model mean. Uncertainty in the value of f for all forcing agents (and possible inter-
 229 model variations in f – see section 7) inhibit a full assessment.

230 We refer to the $k\Delta T_s$ term as the “T-term” and the $-fRF$ term as the “RF-term” although they
 231 could also be termed the “slow” and “fast” responses, respectively, which relates to the
 232 contrasting heat capacities and associated response time-scales of the ocean and atmosphere.
 233 The balance between these two terms varies between climate forcing agents; as will be
 234 shown, they can act to either reinforce or oppose each other. Hence the same ΔT_s from two
 235 different forcing agents can result in a different ΔP .

236 Note the sign convention here. For the case of a positive RF , since k is positive, the effect of
 237 the T-term is to increase R_d as temperature increases – the increased radiative divergence then
 238 leads to a requirement for a greater latent heat flux (and hence an increase in precipitation) to
 239 maintain the tropospheric energy balance; this term provides the direct link between surface
 240 temperature change and precipitation change. If in this same case f (and hence RF_d) is
 241 positive, then the RF-term would oppose the T-term (as it would decrease rather than increase
 242 the radiative divergence) and act to suppress precipitation. Physically, in this case, there is
 243 less “demand” for latent heating to balance the tropospheric energy budget.

244

245

246 **3.2 Illustration for doubling of CO₂**

247 As a simple example of the processes, consider the equilibrium response to a doubling of
 248 carbon dioxide, and take $k = 2.2 \text{ W m}^{-2} \text{ K}^{-1}$ (consistent with the multi-model means in Previdi
 249 (2010) and Thorpe and Andrews (2014)), $RF_{2x \text{ CO}_2} = 3.7 \text{ W m}^{-2}$ (Myhre et al., 2013 who give
 250 the same value for the ERF) and $f = 0.8$ (Andrews et al. 2010). The equilibrium precipitation
 251 change $\Delta P_{2x \text{ CO}_2}$ (in %, assuming a global-mean precipitation of 2.68 mm day^{-1}), can then be
 252 written in terms of the equilibrium surface temperature change $\Delta T_{2x \text{ CO}_2}$ as

$$253 \quad \Delta P_{2x \text{ CO}_2} = 2.79(\Delta T_{2x \text{ CO}_2} - 1.35). \quad (4)$$

254 This equation shows that if $\Delta T_{2x \text{ CO}_2} = 1.35 \text{ K}$, which, via $\Delta T_{2x \text{ CO}_2} = \lambda RF_{2x \text{ CO}_2}$, corresponds to a
 255 climate sensitivity λ of $0.36 \text{ K (W m}^{-2})^{-1}$, $\Delta P_{2x \text{ CO}_2}$ would be zero. The slope of the line is
 256 2.79 \% K^{-1} . Such an expression fits well the intercept and slope of the linear fit to equilibrium
 257 double-CO₂ experiments from a range of climate models found by Allen and Ingram (2002 –
 258 their Fig. 2). Hence Eq. (4) acts as a further validation of the utility of Eq. (3) for simulating
 259 global-mean precipitation change across climate models with varying parameterisations of,
 260 for example, convection, with climate sensitivities varying across the range from about 0.4 to
 261 $1.3 \text{ K (W m}^{-2})^{-1}$. The departures of individual models from this best fit could originate from
 262 differences in any of the values of $k, f, RF_{2x \text{ CO}_2}$ assumed here, or in inter-model differences in
 263 the importance of the fast component of ΔSH which is not accounted for here. The slope of
 264 the line also corresponds to hydrological sensitivity due only to the T-term, and is in good
 265 agreement with the multi-model mean derived by Thorpe and Andrews (2014).

266 Since more generally, $\Delta T_{eq} = \lambda RF_{eq}$, Eq.(3) can also be written in a more general form for any
 267 ΔT_{eq} (and hence RF_{eq}), so that the equilibrium change in precipitation ΔP_{eq} (in %) is given by

$$268 \quad \Delta P_{eq} = 1.3 \Delta T_{eq} (k - f/\lambda). \quad (5)$$

269 This emphasizes that the offset between the T- and RF-terms depends strongly on λ . Using a
 270 mid-range climate sensitivity of $0.8 \text{ K (W m}^{-2})^{-1}$, the RF-term for CO₂ offsets about 50% of
 271 the precipitation change that would result from the T-term alone. Considering the IPCC
 272 (2013) “likely” range for λ , which is 0.4 to $1.2 \text{ K (W m}^{-2})^{-1}$, the RF-term offsets the T-term by
 273 about 90% for low λ and by 30% at high λ . The overall global-mean equilibrium hydrological
 274 sensitivity ($\Delta P_{eq}/\Delta T_{eq}$) to CO₂ forcing can be derived from Eq. (5) and varies from about 0.25
 275 \% K^{-1} to 2 \% K^{-1} over this range of λ , which can be compared with the value of 2.79 \% K^{-1}
 276 due solely to the T-term.

277 **3.3 Application to emissions of a gas or aerosol**

278 To relate the understanding encapsulated in Equation (3) to an emission of a gas or aerosol,
 279 we consider first the GPP for a pulse emission of unit mass of a gas at time $t=0$ and consider

280 the precipitation change at a time H after the emission. Following convention, we label this
281 the Absolute GPP ($AGPP_p$), which is presented here in units of $\text{mm day}^{-1} \text{kg}^{-1}$.

282 The T-term in Eq. (3) becomes k times the absolute GTP_P ($AGTP_p$) (e.g. Shine et al. 2005).
283 Assuming for small perturbations that RF is linear in the concentration of the emitted species,
284 x , and that the perturbation decays exponentially with time constant τ_x , then for a unit
285 emission, the RF-term is given by $-f_x A_x \exp(-H / \tau_x)$, where A_x is the specific RF (in W m^{-2}
286 kg^{-1}) of the emitted species. Hence the $AGPP$ (in $\text{mm day}^{-1} \text{kg}^{-1}$) is given by

$$287 \quad AGPP_p^x(H) = 0.034(kAGTP_p^x(H) - f_x A_x \exp(-H / \tau_x)). \quad (6)$$

288 Since a perturbation of CO_2 does not decay following a simple exponential (see e.g. Joos et
289 al. 2013), the calculation of $AGPP_p^{CO_2}(H)$ is slightly more involved – see the Appendix for
290 more details.

291 The effect of a sustained emission of a unit mass of gas per year, from time $t=0$ can also be
292 considered yielding a sustained $AGPP$ ($AGPP_s$). In this case, the $AGTP_s$ (see Shine et al.
293 2005) can be used for the T-term and the RF-term is now proportional to the time variation of
294 the perturbation of the species to a step-perturbation (e.g. Fuglestedt et al. 2010). The
295 $AGPP_s$ is given by

$$296 \quad AGPP_s^x(H) = 0.034(kAGTP_s^x(H) - f_x A_x \tau_x (1 - \exp(-H / \tau_x))) \quad (7)$$

297 which can also be expressed as a function of both $AGTP_s$ and $AGWP$ as

$$298 \quad AGPP_s^x(H) = 0.034(kAGTP_s^x(H) - f_x AGWP^x(H)) \quad (8)$$

299 The calculation of $AGPP_s^{CO_2}(H)$ is explained in the Appendix. Note that when H is long
300 compared to the time-scale of the climate response (several hundred years in this case – see
301 the Appendix) the $AGTP_s^x(H)$ can itself be related to the $AGWP_p^x(H)$ (see e.g. Shine et al.
302 (2005)) which would simplify Eq. (8) further.

303 Here the $AGPP_p$ and $AGPP_s$ are used to calculate the GPP_p and GPP_s relative to a reference
304 gas, and following common practice for GWP and GTP, CO_2 is used as that reference gas
305 here, although difficulties with this choice will be noted. The GPP_p , relative to an equal mass
306 emission of CO_2 , is then given by

$$307 \quad GPP_p^x(H) = \frac{AGPP_p^x(H)}{AGPP_p^{CO_2}(H)} \quad (8)$$

308 with a similar expression for GPP_s .

309 Note we have chosen to present the $AGPP_p$ and $AGPP_s$ as end-point metrics – i.e. as the
310 effect at the time horizon H of an emission at (or starting at) $t=0$. For some purposes, a time-
311 integrated metric might give a useful perspective. Following Peters et al. (2011 – see in
312 particular its Supplementary Information) we note that time-integrated pulse metrics are

313 mathematically equivalent to end-point metrics for sustained emissions. Hence, the AGPP_S
 314 and GPP_S can equally be interpreted as time-integrated forms of the AGPP_P and GPP_P.

315 **4. Illustrative values for the Absolute Global Precipitation-change Potential**

316 In this section, illustrative calculations of the AGPP are presented. Values for gas lifetimes
 317 and A_x are taken from Myhre et al. (2013) and are described in more detail in the Appendix.
 318 The AGTP calculation requires a representation of the surface temperature response, which
 319 depends on the climate sensitivity and rate of ocean heat uptake. We use the simple impulse-
 320 response function in Boucher and Reddy (2008) (as used in Myhre et al. (2013) for GTP
 321 calculations). Details are given in the Appendix. Values of f , which describe the partitioning
 322 of the RF between surface and atmosphere are taken from Andrews et al. (2010) – these will
 323 likely be quite strongly model dependent, but for illustration purposes, they suffice. Some
 324 sensitivity tests to the representation of the impulse-response function and f are presented in
 325 Section 7. The calculations for CH₄ and N₂O emissions include indirect effects, the most
 326 prominent being their impact on ozone. Different values of f should be used for each indirect
 327 component, but in the absence of robust assessments for these, the same value of f is used for
 328 the indirect components as is used for the direct components.

329 **4.1 Well-mixed greenhouse gases**

330 Figure 1 shows the AGPP_P for CO₂, CH₄ and N₂O, for the total and the RF and T terms
 331 individually, for a period of 100 years after the pulse emission. In Andrews et al. (2010), f is
 332 larger for CO₂ (0.8) than for methane (0.5) because, for present-day concentrations, the lower
 333 opacity of the methane bands means that the surface feels more of the top-of-the-atmosphere
 334 forcing than it does for CO₂. Since N₂O has a similar atmospheric opacity to CH₄, it is
 335 hypothesized that surface-atmosphere partitioning of the RF also behaves in a similar way to
 336 CH₄ and so the value of f for N₂O is also taken to be 0.5; further work is needed to establish
 337 this. Hence, from Eq. (3), the degree of offset between the RF- and T-terms is larger for CO₂
 338 than for CH₄ and N₂O.

339 Figure 1(a) for CO₂ illustrates the general behaviour. For a pulse emission, the size of the RF-
 340 term is maximised at the time of emission, as this is when the concentration is largest, and
 341 then decays as the perturbation decays. The T-term is dictated by the timescale of the
 342 response of the surface temperature to the forcing. The characteristic temperature response to
 343 a pulse forcing (e.g. Shine et al. 2005) is an initial increase in T, as the thermal inertia of the
 344 surface means it takes time to respond to the forcing, reaching a maximum, followed by a
 345 decrease that is controlled by the timescales of both the decay of the pulse and the climate
 346 response. For the first 5 years, the CO₂ precipitation response is negative as the RF-term
 347 dominates, after which the T-term dominates, but the total is approximately 50% of the T-
 348 term. The long perturbation timescales mean that the effect on precipitation persists for more
 349 than 100 years after an emission, as does the competition between the T- and RF-terms.

350 N₂O has a lifetime of the order of a century and its AGPP_P (Fig. 1(b)) is qualitatively similar
 351 to CO₂ but the T-term dominates, because f is smaller. As CH₄ is much shorter lived, its

352 behaviour is somewhat different. As the pulse, and the associated RF, has disappeared by
 353 about year 40, after this time the AGPP_P is determined by the T-term only.

354 **4.2 Short-lived species**

355 The AGPP is illustrated for two short-lived species, sulphate and black carbon (BC) aerosols.
 356 For both cases, the radiative efficiency and lifetime values from Myhre et al. (2013) are used
 357 and given in the Appendix; for these illustration purposes only the sulphate direct effects are
 358 included, and the BC values include some aerosol-cloud interaction and surface albedo
 359 effects. In terms of the surface-atmosphere partitioning of RF, these are two contrasting
 360 cases. For sulphate, the Andrews et al. (2010) model results indicate an f value less than 0.01
 361 in magnitude and is assumed here to be zero; this indicates that essentially all of the top-of-
 362 the-atmosphere forcing reaches the surface. By contrast, Andrews et al. (2010) find that for
 363 BC, f is 2.5, so that RF_a is much greater than RF; the surface forcing is of opposite sign to RF
 364 and RF_a as the surface is deprived of energy, while the atmosphere gains energy. As will be
 365 discussed further in Section 7, there are considerable uncertainties in these values, especially
 366 for BC, where both RF and f depend strongly on the altitude of the BC. Nevertheless, the
 367 values used here suffice to illustrate a number of important points.

368 Figure 2 shows the AGPP_P for BC and sulphate. As both are very short-lived (weeks)
 369 compared to the greenhouse gases, their RF-term decays to zero within a year (and hence is
 370 not visible on Fig. 2), and it is only the thermal inertia of the climate system that enables
 371 them to influence temperature (and hence precipitation) beyond this time period.

372 An alternative perspective is provided for the sustained-emissions case. In this case, because
 373 the BC and sulphate perturbations persist, so too does the influence of the RF-term on
 374 precipitation. Figure 3 shows the AGPP_S for CO₂, BC and sulphate. For CO₂, the long-time
 375 scales of the CO₂ perturbation mean that both the RF term and T term increase throughout the
 376 100 year period shown. At short time-horizons, the RF-term dominates, leading to
 377 suppression of global precipitation, but after about 15 years, the T-term starts to dominate,
 378 and the AGPP_S becomes positive. For BC, the impact of the large RF-term is dramatic. It is
 379 strongly negative and constant with time (because of the short lifetime), while the T term is
 380 positive and increases until the temperature is almost in equilibrium with the RF. This
 381 counteracts the impact of the RF term, but the total nevertheless remains negative throughout.
 382 For sulphate, because f is assumed to be zero, the total remains equal to the T-term.

383 **5. The GPP relative to CO₂**

384 Absolute GPP values were presented in section 4. In this section we normalize the GPP
 385 values to the effects of the reference gas CO₂ to provide a relative measure, using Eq. (9) and
 386 its equivalent for sustained emissions.

387 **5.1 Well-mixed greenhouse gases**

388 Figure 4 shows the GPP_P for N₂O and CH₄; for comparison, the GTP_P is also shown. Note
 389 that the plots start at H=20 years, as the time at which the AGPP_P crosses the zero axis differs
 390 slightly amongst the gases, and this results in a singularity in Eq. (9). For N₂O, the GPP_P is at

391 least 300 times greater than CO₂ on all timescales shown, and, per unit emission, is more than
 392 40% more effective at changing precipitation than temperature (as given by the GTP_P),
 393 compared to CO₂. This is because the RF-term is less effective at muting the T-term for
 394 N₂O's GPP_P than is the case for CO₂. For CH₄ the difference between the GPP_P and GTP_P is
 395 most marked in an absolute sense at shorter time horizons, when the GPP_P of methane is
 396 affected most by the RF-term; the GPP_P and the absolute difference with the GTP decline at
 397 longer time scales when it is entirely due to the difference between the AGTP_P and AGPP_P
 398 for CO₂.

399 Table 1 presents the values of all absolute metrics used here for CO₂ and Table 2 presents the
 400 values of the GWP, GTP_P and GPP_P for H of 20 and 100 years; these time horizons are
 401 chosen for illustrative purposes, rather than being indicative that they have special
 402 significance, except insofar as 100 years is used for the GWP within the Kyoto Protocol (e.g.
 403 Myhre et al. 2013). For CH₄, the GPP_P(20) is 50% larger than the GWP_P(20) and almost
 404 double the GTP_P(20) mostly because of the larger effect of the RF-term on the AGPP_P for
 405 CO₂. The time-integrated nature of the GWP means that it is much higher than the GTP_P and
 406 GPP_P at 100 years, while the GPP_P remains about double the GTP_P. The GPP_P for N₂O is 25-
 407 50% higher than the GWP and GTP_P at both values of H, again because of the larger effect of
 408 the RF-term on the AGPP_P for CO₂.

409 5.2 Short-lived species

410 Figure 5 shows the GPP_P and GTP_P for BC and sulphate. As noted in Section 4.2, the radical
 411 difference in their values of f (2.5 for black carbon, 0 for sulphate) has no impact on the
 412 AGPP_P for BC and sulphate beyond very short timescales. Because of this, in Fig. 5, the only
 413 difference between the GPP_P and GTP_P comes from the influence of the RF-term on $AGPP_P^{CO_2}$
 414 , and on an equal emissions basis both short-lived species are, relative to CO₂, more effective
 415 at changing precipitation than temperature – this is also shown in Table 2.

416 Figure 6 shows the GPP_S, comparing it with the GTP_S. For sulphate, the difference between
 417 the GPP_S and GTP_S originates entirely from the effect of the RF-term on $AGPP_S^{CO_2}$, because
 418 of the assumption that f is zero. For BC they differ dramatically – whilst both BC and CO₂
 419 cause a warming, so that GTP_S is positive, their impact on precipitation is opposite, and the
 420 BC GPP_S is negative.

421 Table 3 presents values of the GTP_S and GPP_S for H = 20 and 100 years, including the values
 422 for CH₄ and N₂O for completeness. The GPP_S values at 20 years are particularly influenced
 423 by the fact that the AGPP_S for CO₂ is relatively small at this time, due to the strong
 424 cancellation between the T and RF terms. At both values of H, GPP_S values are higher in
 425 magnitude than the corresponding GTP_S values for all non-CO₂ components considered here.

426 6. Precipitation response to realistic emissions

427 To illustrate a further usage of the AGPP_P and AGPP_S, Figs. 7 and 8 apply them to 2008
 428 emissions, to examine the consequences of the emissions of the 5 example species on
 429 precipitation. Figure 8.33 of Myhre et al. (2013) presents a similar calculation applying the

430 AGTP_P and shows that the 5 species used here are the dominant emissions for determining
431 temperature change; hence it was felt useful to also present the total effect of the 5 emissions
432 in the figures. Emissions are taken from Table 8.SM.18 of Myhre et al. (2013) and
433 reproduced in Table A.1. For reference, the corresponding values using the AGTP_P and
434 AGTP_S are also shown in the figures.

435 Figure 7 shows the impact of the 2008 emissions, emitted as a single pulse, on global
436 precipitation and temperature change in subsequent years. While the emissions of CH₄,
437 sulphate and BC are 2 to 4 orders of magnitude smaller than those of CO₂, in the early years
438 after the emission, their effects are competitive with CO₂ because of the size of the GPP_P and
439 GTP_P; emissions of N₂O are small enough that, despite its large GPP_P, its absolute
440 contribution remains low throughout. Because of the differing compensations between the T-
441 and RF-terms for CO₂ and CH₄, their relative importance differs quite significantly between
442 precipitation and temperature. Methane's contribution to precipitation change is less negative
443 or more positive than that of CO₂ until about 20 years; it exceeds the CO₂ contribution by a
444 factor of 2 at about 10 years, and remains 25% of the CO₂ effect even at 50 years. For
445 temperature, the contributions are approximately the same until 10 years, after which the CO₂
446 contribution dominates, being about 7 times larger by 50 years. For the two aerosol
447 components, the GPP_P is unaffected by the RF-term (because the RF due to a pulse emission
448 of a short-lived gas declines rapidly - see Section 4) but their importance for precipitation
449 relative to CO₂ is enhanced, because the RF-term acts to suppress the effect of CO₂ on
450 precipitation change. Thus, for example, the BC effect on precipitation is larger than CO₂ out
451 to year 10, compared to year 4 for temperature.

452 Figure 8 shows the effect of assuming sustained emissions at 2008 levels. Although not a
453 plausible future scenario (since, for example, emissions of greenhouse gases are at present
454 continuing to rise) it provides a useful baseline experiment to assess the relative roles of
455 current emissions when their atmospheric burdens are replenished each year. As expected
456 from the AGPP_S values, the role of the short-lived species differs considerably from the pulse
457 case, as the RF-term remains active – in the case of precipitation, BC's effect is now negative
458 throughout. Until about 30 years, the net effect of all 5 emissions is a reduction of
459 precipitation, after which the warming due to CH₄ and CO₂ is sufficient for their T-terms to
460 overwhelm the reduction caused by sulphate (due to its T-term) and BC (due to its RF-term).
461 This near-term reduction of precipitation is also seen in the results of Allan et al. (2014),
462 where the precipitation changes are driven directly by forcings and temperatures (rather than
463 by emissions, as is the case here). By contrast, the temperature effect is positive after year 1.
464 Perhaps most marked is the role of CH₄. It is the dominant driver of positive precipitation
465 change until about year 50 and even after 100 years its effect is about 50% of that due to CO₂.
466 This differs from temperature, where the CO₂ effect is greatest after 15 years and 3 times
467 larger by 100 years. Figure 8 also illustrates the extent to which the sulphate and BC
468 emissions are opposing the precipitation increase due to the greenhouse gases, at large values
469 of H; those components would respond relatively quickly to any changes in emissions.

470 While these are clearly idealised applications of uncertain metrics, they nevertheless illustrate
471 their potential utility for assessing the relative importance over time of different emissions on

472 global precipitation change. The approach could be extended to past or possible future
 473 emission profiles, by convolving the time-dependent emissions with the GPP_P and GPP_S
 474 values.

475 **7. Sensitivities and uncertainties**

476 There are many uncertainties and sensitivities in the calculation of metrics such as
 477 assumptions about the background state (which can affect A_x and τ_x), and the impulse-
 478 response function for CO_2 (see e.g. Fuglestvedt et al. 2010; Joos et al. 2013; Myhre et al.
 479 2013). Two sensitivities are explored. First, the impulse-response model for surface
 480 temperature change used here (see Section 4) is a fit to output from experiments with one
 481 particular climate model with its own particular climate sensitivity. Olivié et al. (2012)
 482 present similar fits derived from 17 different climate models, or model variants - the fits
 483 shown in Table 5 of Olivié et al. (2012) are used, along with the Boucher and Reddy (2008)
 484 fit used in Section 4, and cover a wide range of climate sensitivities (0.49 to $1.06 \text{ K } (W \text{ m}^{-2})^{-1}$)
 485 and timescales of climate response, although we note that model uncertainty range may not
 486 fully straddle the true uncertainty range. Olivié and Peters (2013) used these fits to explore
 487 the sensitivity of the GTP calculations. Figure 9 shows the mean and standard deviation of
 488 the pulse and sustained GTP and GPP derived using these 18 different representations.

489 Considering the absolute pulse metrics for CO_2 , Fig. 9a shows that the $AGTP_P$ is only
 490 moderately sensitive (with a coefficient of variation (cv) of about 20%) to model choice. By
 491 contrast the cv is about 60 and 40% for the $AGPP_P(20)$ and $AGPP_P(100)$, respectively. This is
 492 because the T-term is highly sensitive to the choice of impulse-response model, whilst the
 493 RF-term is independent; hence the degree of compensation between these two terms varies
 494 amongst these models. The GTP_P is most sensitive for short-lived species and this uncertainty
 495 is amplified for the GPP_P , by up to a factor of 2 for the $GPP_P(100)$ for sulphate (Fig. 9d). By
 496 contrast, for the longer-lived species the uncertainty in the GTP_P and GPP_P differ greatly – for
 497 N_2O (Fig. 9c), the cv for GTP_P values is only a percent or so, but is typically 40% for the
 498 GPP_P , as both the numerator and denominator in Eq. (9) are impacted by compensations in
 499 the T- and RF-terms to different degrees at different times.

500 The GPP_S is more sensitive because even the sign of the $AGPP_S^{CO_2}$ is not well constrained at 20
 501 years (Fig. 9a). Roughly half of the impulse-response models yield positive values and half
 502 negative ones, with two near zero, because of the differing degrees of compensation between
 503 the T- and RF-terms. The value of H at which the $AGPP_S^{CO_2}$ is zero varies from 11 to 61 years
 504 amongst the models. (For comparison, for the $AGPP_P^{CO_2}$, the corresponding range is 4 to 13
 505 years.) In these circumstances, it becomes difficult to compare the GPP_S values as they vary
 506 wildly from model to model (from -18000 to 24000 for the $GPP_S(20)$ for N_2O) and for this
 507 reason the $AGPP_S$ is presented in Fig. 9. Even the $AGPP_S^{CO_2}(100)$ values vary by over an
 508 order of magnitude across the 18 models. In general, the uncertainties in the $AGPP_S$ exceed
 509 those in the $AGTP_S$; this is most marked in the case of N_2O , where the GTP_S is almost
 510 insensitive to the choice of impulse-response model, as the effect of this choice on the
 511 $AGTP_S$ for CO_2 and N_2O is almost the same.

512 The second sensitivity explored here is to the assumed values of f by replacing the Andrews
 513 et al. (2010) values by those from Kvalevåg et al. (2013) (see Table 1). Where available, we
 514 use the values of f from the larger forcing perturbations given by Kvalevåg et al. (2013) as
 515 these give a clearer signal. For BC, Kvalevåg et al. (2013) present a range of values, for
 516 perturbations at different altitudes – for example they find a value of f of 6.2 (for 10 times the
 517 model-derived vertical profile of BC in response to present-day emissions) and 13 (when 10
 518 times the present-day burden is placed entirely at 550 hPa); these can be compared to the
 519 Andrews et al. (2010) value of 2.5. The difference results mostly from the semi-direct effect
 520 of BC and clouds; when BC is entirely placed at certain pressures (750 and 650 hPa),
 521 Kvalevåg et al.'s (2013) results indicate that f is particularly poorly constrained, because RF
 522 is close to zero, while RF_a is large and positive. This is an example of where casting Eq. (3)
 523 directly in terms of RF_a rather than RF would be advantageous (see Section 3). It should be
 524 noted that this sensitivity test concerns the impact of BC altitude on f rather than on τ_x and A_x .

525 Table 1 shows the $AGPP_P$ and $AGPP_S$ for CO_2 and Table 4 shows the GPP_P and GPP_S ; these
 526 should be compared with the appropriate columns in Tables 2 and 3 (the GWP, GTP_P and
 527 GTP_S are unaffected by f). For the GPP_P for CH_4 and N_2O , the effect of changing the f values
 528 is rather modest (10-20%) because changes in the numerator and denominator of Eq. (9)
 529 compensate to some extent. For BC and sulphate, changes are entirely dependent on the
 530 change in $AGPP_P^{CO_2}$, as the change in f factor has little influence (see Section 4.2) and hence
 531 changes are correspondingly larger (20-30%).

532 The $AGPP_S^{CO_2}(20)$ (Table 1) is rather sensitive to the change in f because of the degree of
 533 compensation between the T- and RF-terms, and increases by more than a factor of 2 (Table
 534 1). This is the dominant reason why the $GPP_S(20)$ for N_2O and CH_4 decrease by about a
 535 factor of 2. The changes at 100 years are much smaller, nearer 10%. The $AGPP_S$ for the short-
 536 lived species are, unlike the $AGPP_P$, now affected by the change in f . Table 5 shows the effect
 537 on the sulphate $GPP_S(20)$ to be about a factor of 2, while the $GPP_S(100)$ is little affected. By
 538 contrast, the GPP_S for black carbon at both time horizons depends significantly on the
 539 altitude of the black carbon perturbation.

540 8. Discussion and Conclusions

541 This paper has used a simple, but demonstrably useful, conceptual model of the drivers of
 542 global-mean precipitation change in response to the imposition of a radiative forcing, to relate
 543 precipitation change directly to emissions. The GPP_P and GPP_S metrics illustrate the interplay
 544 between the two drivers (the atmospheric component of the radiative forcing, and the surface
 545 temperature change) for different forcings, at different time horizons, and for both pulse and
 546 sustained emissions. The GPP_P and GPP_S are given as the change at a specific time horizon
 547 (and hence are end-point metrics). There may be climate effects related to the total change in
 548 precipitation over time for which an integrated metric would be appropriate, so it is useful to
 549 note that the GPP_S can also be interpreted as the time-integrated GPP_P .

550 It has been shown that relative to CO_2 , the pulse and sustained GPP values for the non- CO_2
 551 species examined here are larger than the corresponding GTP values, because the CO_2 GPP is

552 the sum of two quite strongly opposing terms. Further, for black carbon emissions, while
553 they act to warm the climate system, they also act to reduce global-mean precipitation; while
554 this has been clear from the modelling literature for some time, the present work shows how
555 the perspective is different for pulse and sustained emissions. The reduction of precipitation
556 is driven entirely by the radiative forcing component and since, for pulse emissions of short-
557 lived species this falls away on time scales of weeks, it is only apparent on longer time-scales
558 for the sustained perspective. This is an example of how the perturbation design can have a
559 large impact on the calculated response.

560 The evaluation of precipitation metrics assumes that the parameters required for the simple
561 conceptual model are available, and in particular the partitioning of radiative forcing between
562 surface and atmosphere. Only a rather limited number of model studies of this partitioning
563 are currently available, and there are significant differences amongst these and particular
564 sensitivity to the altitude of absorbing aerosol (e.g. Ming et al. (2010), Kvalevåg et al.
565 (2013)). In addition, further development of the simple conceptual model (particularly to
566 account for fast changes in the sensible heat flux) would be beneficial, once understanding
567 improves, as would a fully consistent usage of effective radiative forcings. The ongoing
568 Precipitation Driver Response Model Intercomparison Project (PDRMIP)
569 (<http://cicero.uio.no/PDRMIP/>) should provide important information on the utility of the
570 conceptual model and of the degree of robustness of the surface-atmosphere partitioning
571 amongst a range of climate models for a number of radiative forcing mechanisms. Clearly
572 further studies for a wider range of forcing agents are also needed and indeed casting Eq. (3)
573 directly in terms of the atmospheric component of radiative forcing RF_a (rather than top-of-
574 atmosphere radiative forcing) would be desirable if values of RF_a become more readily
575 available.

576 It is not suggested that the new metrics could replace conventional emissions metrics such as
577 the GWP and GTP in climate policy or emission trading contexts, but they do provide a
578 useful additional perspective for assessing the effects of emissions; they particularly help to
579 emphasise where the impact on precipitation differs significantly from that on temperature or
580 forcing. One difficulty in its application is that conventional metrics generally use CO₂ as a
581 reference gas. For precipitation change, the forcing and surface temperature components
582 oppose each other, which means that the effect of CO₂ emissions on precipitation can be zero
583 (at least in the global-mean) at short time horizons for both pulse and sustained emissions.
584 This is clearly undesirable for a reference gas, and it has also been shown that the timing of
585 this zero point is rather sensitive to the particular parameters used in its calculation. Hence
586 absolute metrics may be more instructive. By applying the absolute metrics to a specific
587 illustrative case (emissions in 2008, either as a pulse, or sustained indefinitely) the
588 importance of methane in influencing the global-mean precipitation change is highlighted –
589 using the default model parameters here, in the sustained 2008 emissions case, the
590 precipitation change from methane exceeds that from CO₂ for about 50 years, By contrast, for
591 temperature, the effect of CO₂ emissions are almost immediately at least comparable to, or
592 stronger than, methane.

593 It has been stressed that use of global-mean precipitation change as a measure of impact has
594 difficulties, because predicted future changes differ in sign between regions – the global-
595 mean is a small residual of these opposing more localised changes and hence it only gives
596 rather general guidance on the effect of different drivers on the changing hydrological cycle.
597 Nevertheless, some of the regional pattern of response can be understood as a generic and
598 coherent response to temperature change. Increases and decreases in precipitation are largely
599 reflective of an amplification of precipitation minus evaporation fields, primarily explained
600 by increasing concentrations of water vapour with warming (as expected from the Clausius-
601 Clapeyron equation); this leads to systematic increases and decreases in precipitation
602 depending on the region (e.g. Held and Soden, 2006, Liu and Allan 2013).

603 The approach here could be enhanced to a more regional level of response by either using a
604 simple pattern-scaling approach (whereby the pattern of predicted precipitation change scales
605 with the global-mean) or, better, to derive a regional variation that accounts for the different
606 effects of the forcing and temperature response on precipitation change (Good et al. 2012).
607 The patterns emerging from such an approach would likely depend significantly on which
608 climate model was used to derive them. In addition, such patterns would be needed for all the
609 primary forcing agents. For short-lived emissions, it is known that even global-mean metrics
610 such as the GWP and GTP depend on the emission location (e.g., Fuglestvedt et al. 2010) –
611 this will also be true for the precipitation metrics. Metrics can also be posed in terms of the
612 regional response to regional emissions. For example, Collins et al. (2013) employed the
613 Regional Temperature Potential proposed by Shindell (2012) whereby a matrix is produced
614 that characterises the effect of RFs in a set of given regions on the temperature change in a set
615 of given regions; a similar approach could be taken using the Regional Precipitation Potential
616 proposed by Shindell et al. (2012).

617 In spite of the difficulties in quantifying the precipitation metrics given present knowledge of
618 the driving parameters, the framework presented here adds a useful extra dimension to simple
619 tools that are currently available for assessing the impact of emissions of different gases and
620 particulates.

621 **Author contribution:** KPS conceived the idea of the emissions metrics for precipitation,
622 through conversations with RPA, performed the calculations and led the writing. RPA, WJC
623 and JSF provided major critical input to the drafts, including ideas on adjusting the emphasis
624 of the paper and on possible applications of the metrics.

625 **Acknowledgements:** We acknowledge funding from the European Commission, under the
626 ECLIPSE (Evaluating the Climate and Air Quality Impacts of Short-Lived Pollutants) Project
627 (Grant Agreement 282688) and thank other ECLIPSE partners for their encouragement and
628 input to this work. We are grateful to Katsumasa Tanaka, an anonymous reviewer and the
629 Editor, Steven Smith, for their helpful comments, and for suggestions and input from
630 participants in PDRMIP.

631 **Appendix**

632 The impulse response function, $R(t)$, for a pulse emission of CO₂ is assumed to be of the
633 form

$$634 \quad R(t) = a_0 + \sum_{j=1}^3 a_j \exp\left(-\frac{t}{\alpha_j}\right) \quad (\text{A1})$$

635 where the parameters used here follow Myhre et al. (2013), with $a_0=0.2173$, $a_1=0.2240$,
636 $a_2=0.2824$, $a_3=0.2763$ and $\alpha_1= 394.4$ years, $\alpha_2= 36.54$ years and $\alpha_3= 4.304$ years.

637 The impulse response function for global-mean surface temperature in Sections 4 to 6 is
638 taken from Boucher and Reddy (2008) and is of the form

$$639 \quad R(t) = \sum_{i=1}^2 \frac{c_i}{d_i} \exp\left(-\frac{t}{d_i}\right) \quad (\text{A2})$$

640 with $c_1=0.631 \text{ K (W m}^{-2}\text{)}^{-1}$, $c_2=0.429 \text{ K (W m}^{-2}\text{)}^{-1}$ and $d_1=8.4$ years and $d_2=409.5$ years. The
641 equilibrium climate sensitivity for this function is $1.06 \text{ K (W m}^{-2}\text{)}^{-1}$, equivalent to an
642 equilibrium surface temperature change for a doubling of CO₂ of about 3.9 K. Additional
643 impulse-response functions are used in Section 7, with alternative values of c_i and d_i .

644 To derive the AGPP_P in Eq. (6), for species for which the perturbation decays exponentially
645 with a single time-constant τ_x , an expression for AGTP_P is required. For a species with a
646 specific RF A_x and using Eq. (A2) this is given by (see, for example, Fuglestedt et al.
647 (2010))

$$648 \quad AGTP_P^x(t) = A_x \tau_x \sum_{i=1}^2 \frac{c_i}{\tau_x - d_i} (\exp(-t / \tau_x) - \exp(-t / d_i)). \quad (\text{A3})$$

649 This equation does not apply in the case where $\tau_x = d_i$; the appropriate expression is given in
650 Shine et al. (2005) for this case, which has to be modified for the two-term form of Eq. (A2).

651 For the case of CO₂, where the decay of a pulse is given by Eq. (A1), the AGTP_P is given by
652 (see, for example, Fuglestedt et al. (2010))

$$653 \quad AGTP_P^{CO_2}(t) = A_{CO_2} \left[a_0 \sum_{i=1}^2 c_i (1 - \exp(-\frac{t}{d_i})) + \sum_{i=1}^2 c_i \sum_{j=1}^3 \frac{a_j \alpha_j}{\alpha_j - d_i} (\exp(-t / \alpha_j) - \exp(-t / d_i)) \right], \quad (\text{A4})$$

654 and the exponential in the second term on the right-hand side of Eq. (6) is replaced by Eq.
655 (A1).

656 To derive the AGPP_S in Eq. (7), the GTP_S for non-CO₂ species is given by (by rearranging
657 the expression in Shine et al. (2005) following Peters et al. (2011))

658
$$AGTP_S^x(t) = A_x \tau_x \left[\sum_{i=1}^2 \frac{c_i}{\tau_x - d_i} (\tau_x (1 - \exp(-t / \tau_x)) - d_i (1 - \exp(-t / d_i))) \right] \quad (A5)$$

659 and again the case where $\tau_x = d_i$ is given in Shine et al. (2005), which has to be modified for
 660 the two-term form of Eq. (A2).

661 The calculation of the $AGPP_S$ for CO_2 requires the $AGTP_S$ and is given by

662
$$AGTP_S^{CO_2}(t) = \sum_{i=1}^2 A_{CO_2} c_i \left[a_o (t - d_i (1 - \exp(-t / d_i))) + \sum_{j=1}^3 \frac{\alpha_j a_j}{\alpha_j - d_i} (\alpha_j (1 - \exp(-t / \alpha_j)) - d_i (1 - \exp(-t / d_i))) \right]$$

 663 (A6)

664 and also $AGWP^{CO_2}$, for the second term on the right hand side of Eq. (7) which is

665
$$AGWP^{CO_2}(t) = A_{CO_2} (a_o t + \sum_{j=1}^3 a_j \alpha_j (1 - \exp(-\frac{t}{\alpha_j}))) \quad . \quad (A7)$$

666 The parameters used for the 5 different species employed here are presented in Table A1.

667 **References**

- 668 Allan, R. P., Liu, C. L., Zahn, M., Lavers, D. A., Koukouvagias, E., and Bodas-Salcedo, A.:
 669 Physically consistent responses of the global atmospheric hydrological cycle in models and
 670 observations, *Surveys in Geophysics*, 35, 533-552, 10.1007/s10712-012-9213-z, 2014.
- 671 Allen, M. R., and Ingram, W. J.: Constraints on future changes in climate and the hydrologic
 672 cycle, *Nature*, 419, 224-232, 10.1038/nature01092, 2002.
- 673 Andrews, T., Forster, P.M., and Gregory J.M.: A surface energy perspective on climate
 674 change, *Journal of Climate*, 22, 2570-2557, 10.1175/2008JCLI2759.1, 2009
- 675 Andrews, T., Forster, P. M., Boucher, O., Bellouin, N., and Jones, A.: Precipitation, radiative
 676 forcing and global temperature change, *Geophysical Research Letters*, 37, L14701,
 677 10.1029/2010gl043991, 2010.
- 678 Azar, C., and Johansson, D. J. A.: On the relationship between metrics to compare
 679 greenhouse gases the case of IGTP, GWP and SGTP, *Earth System Dynamics*, 3, 139-147,
 680 10.5194/esd-3-139-2012, 2012.
- 681 Berntsen, T., Fuglestedt, J., Joshi, M., Shine, K., Stuber, N., Ponater, M., Sausen, R.,
 682 Hauglustaine, D., and Li, L.: Response of climate to regional emissions of ozone
 683 precursors: sensitivities and warming potentials, *Tellus Series B-Chemical and Physical
 684 Meteorology*, 57, 283-304, 10.1111/j.1600-0889.2005.00152.x, 2005.
- 685 Boucher, O., and Reddy, M. S.: Climate trade-off between black carbon and carbon dioxide
 686 emissions, *Energy Policy*, 36, 193-200, 10.1016/j.enpol.2007.08.039, 2008.
- 687 Collins, M., Knutti, R., Arblaster, J., Dufresne, J.-L., Fichet, T., Friedlingstein, P., Gao, X.,
 688 Gutowski, W.J., Johns, T., Krinner, G., Shongwe, M., Tebaldi, C., Weaver, A.J., and
 689 Wehner, M.: Long-term Climate Change: Projections, Commitments and Irreversibility, in:
 690 *Climate Change 2013: The Physical Science Basis. Contribution of Working Group I to the
 691 Fifth Assessment Report of the Intergovernmental Panel on Climate Change*, edited by:
 692 Stocker, T. F., Qin, D., Plattner, G. K., Tignor, M., Allen, S. K., Boschung, J., Nauels, A.,
 693 Xia, Y., Bex, V., and Midgley, P. M., Cambridge University Press, Cambridge, United
 694 Kingdom and New York, NY, USA, 659–740, 2013.
- 695 Collins, W. J., Fry, M. M., Yu, H., Fuglestedt, J. S., Shindell, D. T., and West, J. J.: Global
 696 and regional temperature-change potentials for near-term climate forcings, *Atmospheric
 697 Chemistry and Physics*, 13, 2471-2485, 10.5194/acp-13-2471-2013, 2013.
- 698 Deuber, O., Luderer, G., and Sausen, R.: CO₂ equivalences for short-lived climate forcings,
 699 *Climatic Change*, 122, 651-664, 10.1007/s10584-013-1014-y, 2014.
- 700 Fuglestedt, J. S., Shine, K. P., Berntsen, T., Cook, J., Lee, D. S., Stenke, A., Skeie, R. B.,
 701 Velders, G. J. M., and Waitz, I. A.: Transport impacts on atmosphere and climate: Metrics,
 702 *Atmospheric Environment*, 44, 4648-4677, 10.1016/j.atmosenv.2009.04.044, 2010.
- 703 Gillett, N. P., and Matthews, H. D.: Accounting for carbon cycle feedbacks in a comparison
 704 of the global warming effects of greenhouse gases, *Environmental Research Letters*, 5,
 705 034011, 10.1088/1748-9326/5/3/034011, 2010.
- 706 Good, P., Ingram, W., Lambert, F. H., Lowe, J. A., Gregory, J. M., Webb, M. J., Ringer, M.
 707 A., and Wu, P. L.: A step-response approach for predicting and understanding non-linear
 708 precipitation changes, *Climate Dynamics*, 39, 2789-2803, 10.1007/s00382-012-1571-1,
 709 2012.
- 710 Held, I. M., and Soden, B. J.: Robust responses of the hydrological cycle to global warming,
 711 *Journal of Climate*, 19, 5686-5699, 10.1175/jcli3990.1, 2006.
- 712 Huffman, G. J., Adler, R. F., Bolvin, D. T., and Gu, G. J.: Improving the global precipitation
 713 record: GPCP Version 2.1, *Geophysical Research Letters*, 36, L17808,
 714 10.1029/2009gl040000, 2009.
- 715 IPCC: *Climate Change 2013: The Physical Science Basis. Contribution of Working Group I*

- 716 to the Fifth Assessment Report of the Intergovernmental Panel on Climate Change,
717 Cambridge University Press, Cambridge, United Kingdom and New York, NY, USA, 1535
718 pp., 2013.
- 719 Johansson, D. J. A.: Economics- and physical-based metrics for comparing greenhouse gases,
720 *Climatic Change*, 110, 123-141, 10.1007/s10584-011-0072-2, 2012.
- 721 Joos, F., Roth, R., Fuglestedt, J. S., Peters, G. P., Enting, I. G., von Bloh, W., Brovkin, V.,
722 Burke, E. J., Eby, M., Edwards, N. R., Friedrich, T., Frölicher, T. L., Halloran, P. R.,
723 Holden, P. B., Jones, C., Kleinen, T., Mackenzie, F. T., Matsumoto, K., Meinshausen, M.,
724 Plattner, G.-K., Reisinger, A., Segschneider, J., Shaffer, G., Steinacher, M., Strassmann, K.,
725 Tanaka, K., Timmermann, A., and Weaver, A. J.: Carbon dioxide and climate impulse
726 response functions for the computation of greenhouse gas metrics: a multi-model analysis,
727 *Atmos. Chem. Phys.*, 13, 2793-2825, doi:10.5194/acp-13-2793-2013, 2013.
- 728 Knutti, R., and Sendláček, J.: Robustness and uncertainties in the new CMIP5 climate model
729 projections, *Nature Climate Change*, 3, 369-373, 10.1038/nclimate1716, 2013.
- 730 Kvalevag, M. M., Samset, B. H., and Myhre, G.: Hydrological sensitivity to greenhouse
731 gases and aerosols in a global climate model, *Geophysical Research Letters*, 40, 1432-1438,
732 10.1002/grl.50318, 2013.
- 733 Lambert, F. H., and Webb, M. J.: Dependency of global mean precipitation on surface
734 temperature, *Geophysical Research Letters*, 35, L16706, 10.1029/2008gl034838, 2008.
- 735 Liu, C. L., and Allan, R. P.: Observed and simulated precipitation responses in wet and dry
736 regions 1850-2100, *Environmental Research Letters*, 8, 034002, 10.1088/1748-
737 9326/8/3/034002, 2013.
- 738 Ming, Y., Ramaswamy, V., and Persad, G.: Two opposing effects of absorbing aerosols on
739 global-mean precipitation, *Geophysical Research Letters*, 37, L13701,
740 10.1029/2010gl042895, 2010.
- 741 Mitchell, J. F. B., Wilson, C. A., and Cunningham, W. M.: On CO₂ climate sensitivity and
742 model dependence of results, *Quarterly Journal of the Royal Meteorological Society*, 113,
743 293-322, 10.1002/qj.49711347517, 1987.
- 744 Myhre, G., Shindell, D., Bréon, F.-M., Collins, W., Fuglestedt, J., Huang, J., Koch, D.,
745 Lamarque, J.-F., Lee, D., Mendoza, B., Nakajima, T., Robock, A., Stephens, G., Takemura,
746 T., and Zhang, H.: Anthropogenic and Natural Radiative Forcing, in: *Climate Change 2013:
747 The Physical Science Basis. Contribution of Working Group I to the Fifth Assessment
748 Report of the Intergovernmental Panel on Climate Change*, edited by: Stocker, T. F., Qin,
749 D., Plattner, G. K., Tignor, M., Allen, S. K., Boschung, J., Nauels, A., Xia, Y., Bex, V., and
750 Midgley, P. M., Cambridge University Press, Cambridge, United Kingdom and New York,
751 NY, USA, 659–740, 2013.
- 752 O’Gorman, P. A., Allan, R. P., Byrne, M. P., and Previdi, M.: Energetic constraints on
753 precipitation under climate change, *Surveys in Geophysics*, 33, 585-608, 10.1007/s10712-
754 011-9159-6, 2012.
- 755 Olivie, D. J. L., Peters, G. P., and Saint-Martin, D.: Atmosphere response time scales
756 estimated from AOGCM experiments, *Journal of Climate*, 25, 7956-7972, 10.1175/jcli-d-
757 11-00475.1, 2012.
- 758 Olivie, D. J. L., and Peters, G. P.: Variation in emission metrics due to variation in CO₂ and
759 temperature impulse response functions, *Earth System Dynamics*, 4, 267-286, 10.5194/esd-
760 4-267-2013, 2013.
- 761 Peters, G. P., Aamaas, B., Berntsen, T., and Fuglestedt, J. S.: The integrated global
762 temperature change potential (iGTP) and relationships between emission metrics,
763 *Environmental Research Letters*, 6, 044021, 10.1088/1748-9326/6/4/044021, 2011.
- 764 Pierrehumbert, R. T.: Short-lived climate pollution, *Annual Review of Earth and Planetary
765 Sciences*, 42, 341-379, 10.1146/annurev-earth-060313-054843, 2014.

- 766 Previdi, M.: Radiative feedbacks on global precipitation, *Environmental Research Letters*, 5,
767 025211, 10.1088/1748-9326/5/2/025211, 2010.
- 768 Reisinger, A., Havlik, P., Riahi, K., van Vliet, O., Obersteiner, M., and Herrero, M.:
769 Implications of alternative metrics for global mitigation costs and greenhouse gas emissions
770 from agriculture, *Climatic Change*, 117, 677-690, 10.1007/s10584-012-0593-3, 2013.
- 771 Shindell, D. T.: Evaluation of the absolute regional temperature potential, *Atmospheric*
772 *Chemistry and Physics*, 12, 7955-7960, 10.5194/acp-12-7955-2012, 2012.
- 773 Shindell, D. T., Voulgarakis, A., Faluvegi G., and Milly, G.: Precipitation response to
774 regional radiative forcing. *Atmospheric Chemistry and Physics*, 12, 6969-6982,
775 10.5194/acp-12-6969-2012, 2012.
- 776 Shine, K. P., Fuglestedt, J. S., Hailemariam, K., and Stuber, N.: Alternatives to the global
777 warming potential for comparing climate impacts of emissions of greenhouse gases,
778 *Climatic Change*, 68, 281-302, 10.1007/s10584-005-1146-9, 2005.
- 779 Shine, K. P., Berntsen, T. K., Fuglestedt, J. S., Skeie, R. B., and Stuber, N.: Comparing the
780 climate effect of emissions of short- and long-lived climate agents, *Philosophical*
781 *Transactions of the Royal Society A - Mathematical Physical and Engineering Sciences*,
782 365, 1903-1914, 10.1098/rsta.2007.2050, 2007.
- 783 Sterner, E., Johansson, D. A., and Azar, C.: Emission metrics and sea level rise, *Climatic*
784 *Change*, 127, 335-351, 10.1007/s10584-014-1258-1, 2014.
- 785 Strefler, J., Luderer, G., Aboumahboub, T., and Kriegler, E.: Economic impacts of alternative
786 greenhouse gas emission metrics: a model-based assessment, *Climatic Change*, 125, 319-
787 331, 10.1007/s10584-014-1188-y, 2014.
- 788 Takahashi, K.: The global hydrological cycle and atmospheric shortwave absorption in
789 climate models under CO₂ forcing, *Journal of Climate*, 22, 5667-5675,
790 10.1175/2009jcli2674.1, 2009.
- 791 Tanaka, K., O'Neill, B.C., Rokityanskiy, D., Obersteiner, M., and Tol, R.S.J.: Evaluating
792 global warming potentials with historical temperature. *Climatic Change*, 96, 443-466,
793 10.1007/s10584-009-9566-6, 2009.
- 794 Thorpe, L., and Andrews, T.: The physical drivers of historical and 21st century global
795 precipitation changes, *Environmental Research Letters*, 9, 064024, 10.1088/1748-
796 9326/9/6/064024, 2014.
- 797 Tol, R. S. J., Berntsen, T. K., O'Neill, B. C., Fuglestedt, J. S., and Shine, K. P.: A unifying
798 framework for metrics for aggregating the climate effect of different emissions,
799 *Environmental Research Letters*, 7, 044006, 10.1088/1748-9326/7/4/044006, 2012.

800 Table 1. Absolute metrics, AGWP, AGTP_P, AGTP_S, AGPP_P and AGPP_S for CO₂ at time
 801 horizons of 20 and 100 years, which are chosen for illustrative purposes. The first and second
 802 sets of AGPP values use the CO₂ *f* factor from Andrews et al. (2010) and Kvalevåg et al.
 803 (2013) respectively (see Table A1).

	unit	Time horizon (years)	
		20	100
AGWP	W m ⁻² kg ⁻¹ year	2.50 x 10 ⁻¹⁴	9.19 x 10 ⁻¹⁴
AGTP _P	K kg ⁻¹	6.85 x 10 ⁻¹⁶	5.48 x 10 ⁻¹⁶
AGTP _S	K kg ⁻¹ year	1.05 x 10 ⁻¹⁴	5.90 x 10 ⁻¹⁴
AGPP _P (Andrews)	mm day ⁻¹ kg ⁻¹	2.27 x 10 ⁻¹⁷	2.13 x 10 ⁻¹⁷
AGPP _S (Andrews)	mm day ⁻¹ kg ⁻¹ year	1.05 x 10 ⁻¹⁶	1.91 x 10 ⁻¹⁵
AGPP _P (Kvalevåg)	mm day ⁻¹ kg ⁻¹	2.99 x 10 ⁻¹⁷	2.63 x 10 ⁻¹⁷
AGPP _S (Kvalevåg)	mm day ⁻¹ kg ⁻¹ year	2.75 x 10 ⁻¹⁶	2.53 x 10 ⁻¹⁵

804

805 Table 2: The GWP, GTP_P and GPP_P, relative to CO₂, for pulse emissions of 4 species at time
806 horizons of 20 and 100 years, which are chosen for illustrative purposes. The absolute values
807 of metrics for CO₂ are given in Table 1.

	GWP(20)	GWP(100)	GTP _P (20)	GTP _P (100)	GPP _P (20)	GPP _P (100)
CH ₄	84	28	67	4.3	120	8.1
N ₂ O	263	264	276	234	396	325
Sulphate	-141	-38	-41	-5.28	-92	-10.1
Black carbon	2415	657	701	91	1580	173

808

809 Table 3. The GTP_S and GPP_S , relative to CO_2 , for sustained emissions of 4 other species at
810 time horizons of 20 and 100 years, which are chosen for illustrative purposes. The absolute
811 values of metrics for CO_2 are given in Table 1.

	$GTP_S(20)$	$GTP_S(100)$	$GPP_S(20)$	$GPP_S(100)$
CH_4	93	31.5	357	49.6
N_2O	256	267	846	401
Sulphate	-199	-43.2	-1490	-100
Black carbon	3410	741	-23500	-979

812

813 Table 4: The GPP_P and GPP_S , relative to CO_2 , for pulse emissions of 4 other species at time
 814 horizons of 20 and 100 years, which are chosen for illustrative purposes, using the values of
 815 surface-atmosphere partitioning of radiative forcing from Kvalevåg et al. (2013). The two
 816 black carbon values are, respectively, using values of f for a model-derived vertical profile for
 817 present-day emissions and assuming that the present-day burden is placed entirely at 550 hPa.
 818 The absolute values of metrics for CO_2 are given in Table 1.

	$GPP_P(20)$	$GPP_P(100)$	$GPP_S(20)$	$GPP_S(100)$
CH_4	101	6.6	187	44.4
N_2O	370	303	486	367
Sulphate	-70	-8.2	-741	-94.0
Black Carbon	1200	141	-36600, -87400	-3740, -9250

819

820 Table A1: Parameter values used for each species included in calculations. All values are
 821 taken from Myhre et al. (2013), unless otherwise stated, and the CH₄ and N₂O values of A_x
 822 include the indirect effects described there.

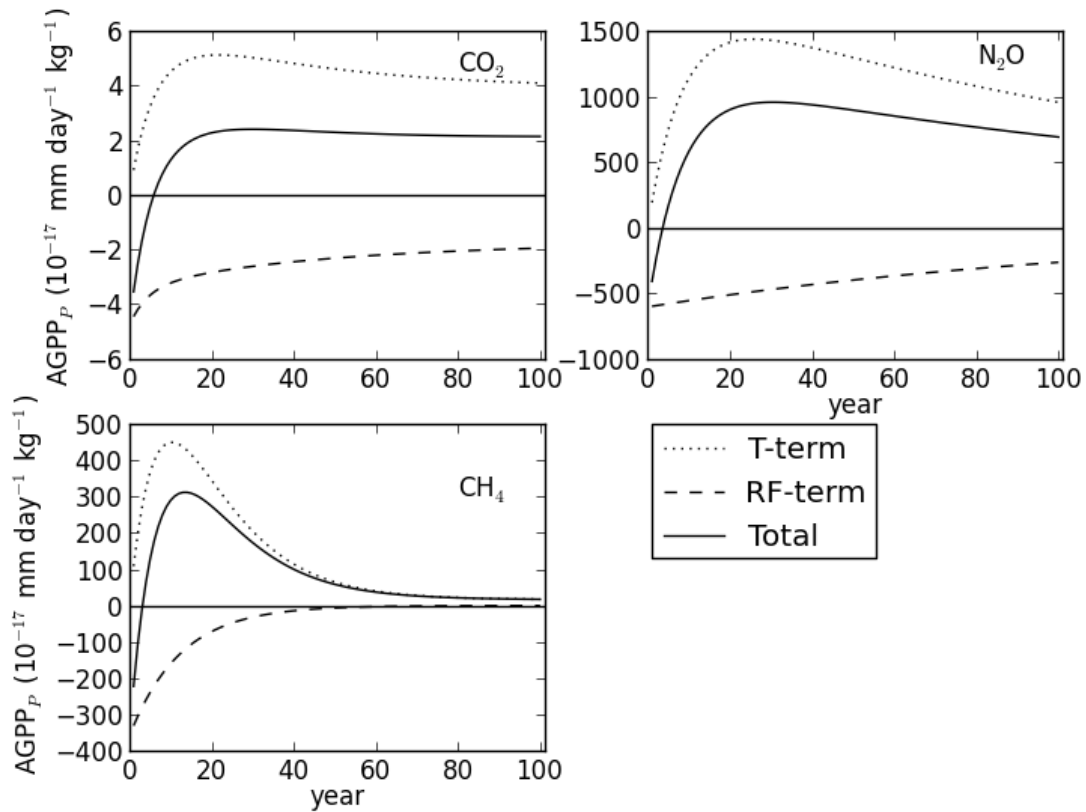
	A _x (W m ⁻² kg ⁻¹)	τ _x (years)	f (Andrews et al. 2010)	f (Kvalevåg et al. 2013)	2008 emissions (kg)
CO ₂	1.76 x 10 ⁻¹⁵	See text	0.8	0.6	3.69 x 10 ¹³
CH ₄	2.11 x 10 ⁻¹³	12.4	0.5	0.3	3.64 x 10 ¹¹
N ₂ O	3.57 x 10 ⁻¹³	121.0	0.5	0.3	1.07 x 10 ¹⁰
Sulphate	-3.2 x 10 ⁻¹⁰	0.011	0.0	-0.4	1.27 x 10 ¹¹
Black carbon	3.02 x 10 ⁻⁹	0.02	2.5	6.2, 13.0	5.31 x 10 ⁹

823

824

825 **Figures**

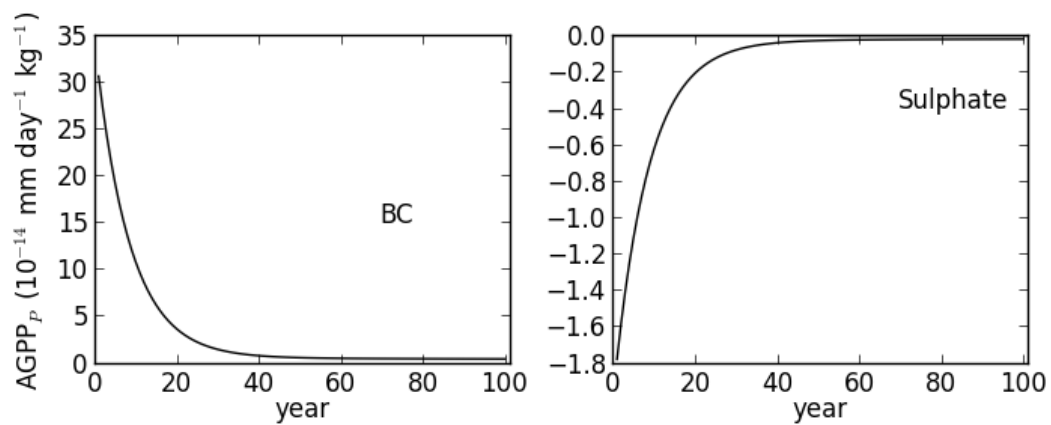
826



827

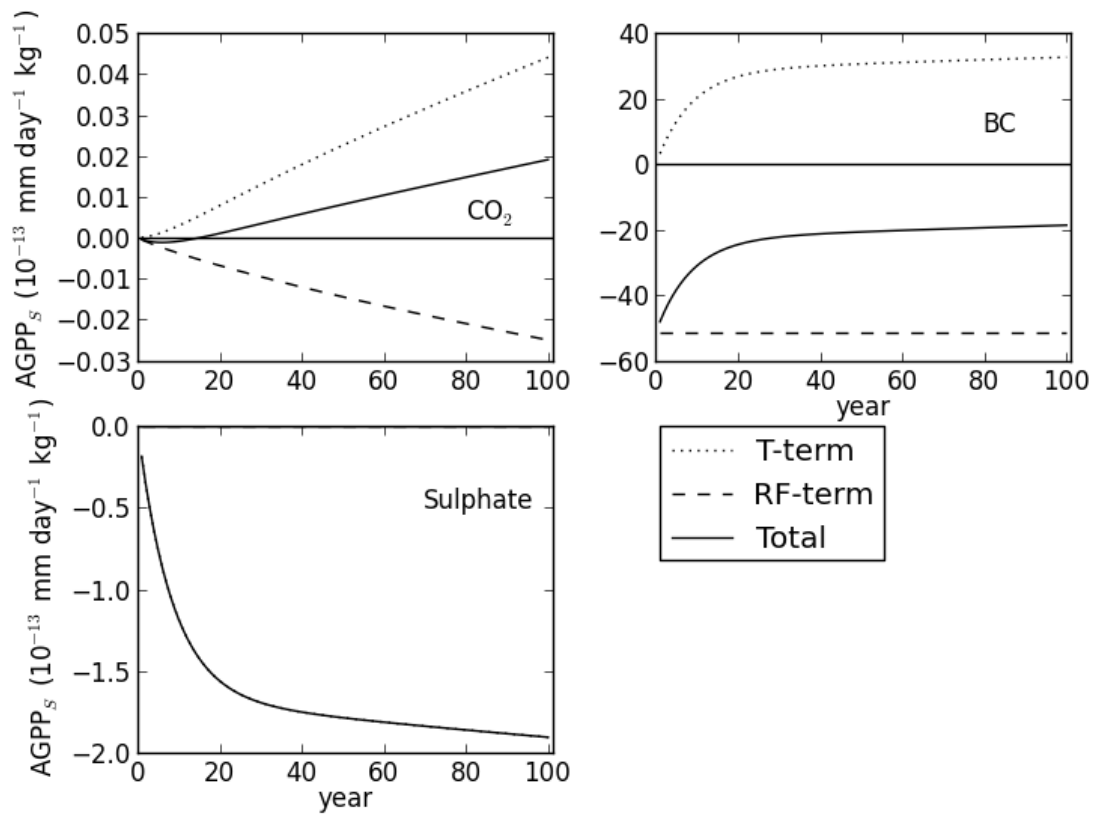
828 Figure 1: AGPP_P for 1 kg pulse emissions of CO_2 , N_2O and CH_4 . The T-term and RF-term
 829 refer to the first and second terms on the right hand side of Eq. (3) respectively, and the Total
 830 is the sum of these.

831



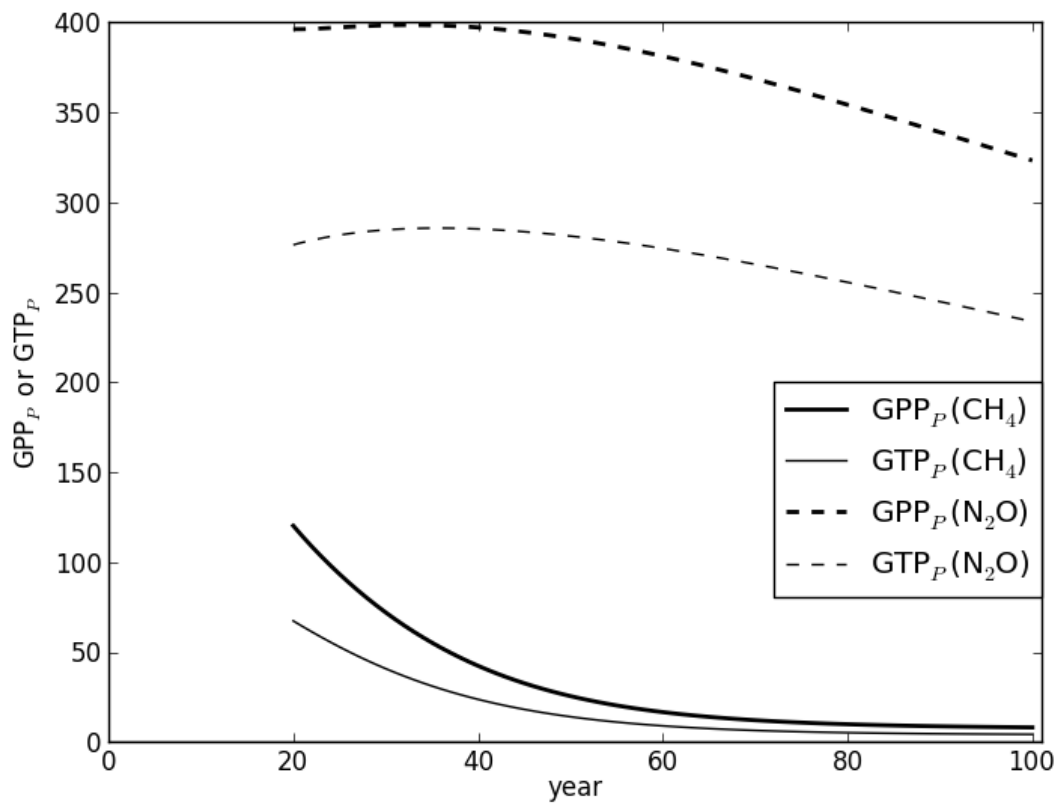
832

833 Figure 2: AGPP_P for 1 kg pulse emissions of black carbon (BC) and sulphate. Note that the
834 RF-term in Eq. (3) is negligible for such short-lived gases, except at time horizons less than a
835 few weeks, and only the total is shown.



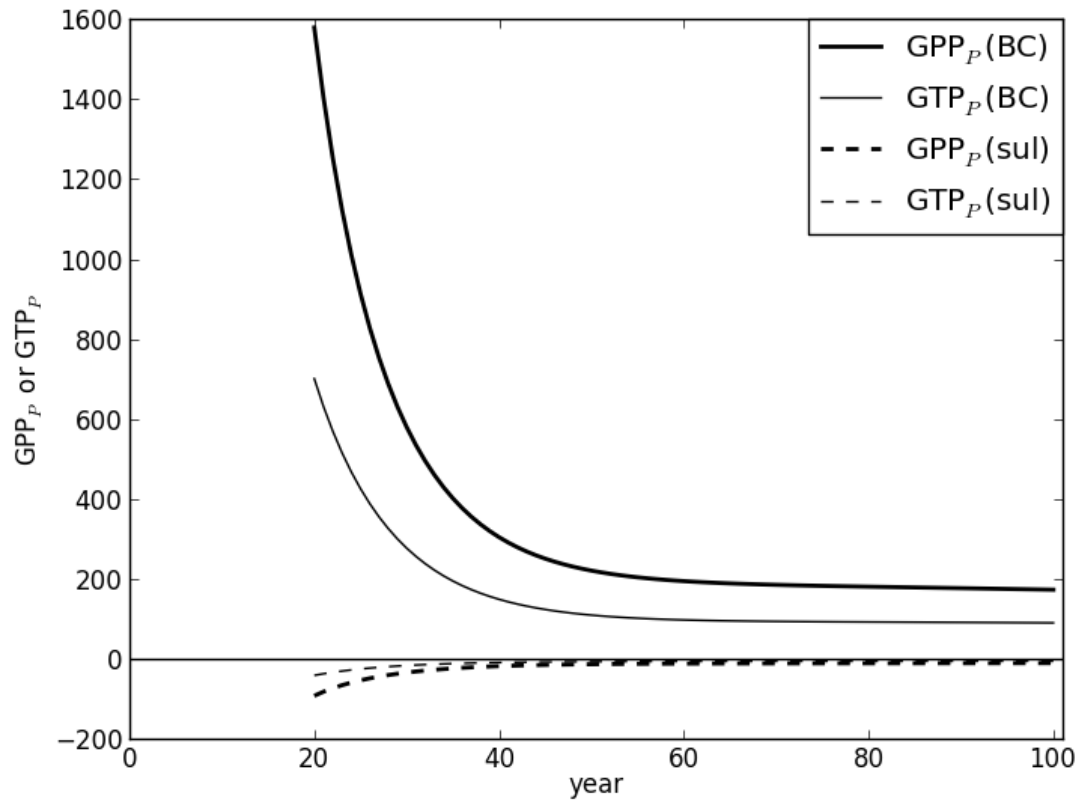
836

837 Figure 3: AGPPs for 1 kg year^{-1} sustained emissions of CO_2 , BC and sulphate. The T-term
 838 and RF-term refer to the first and second terms on the right hand side of Eq. (3) respectively,
 839 and the Total is the sum of these. For sulphate, the RF-term is assumed to be zero (see text)
 840 and so only the Total is shown.



841

842 Figure 4: GPP_P (in bold) and GTP_P for 1 kg pulse emissions of N₂O and CH₄ relative to a 1
843 kg pulse emission of CO₂.

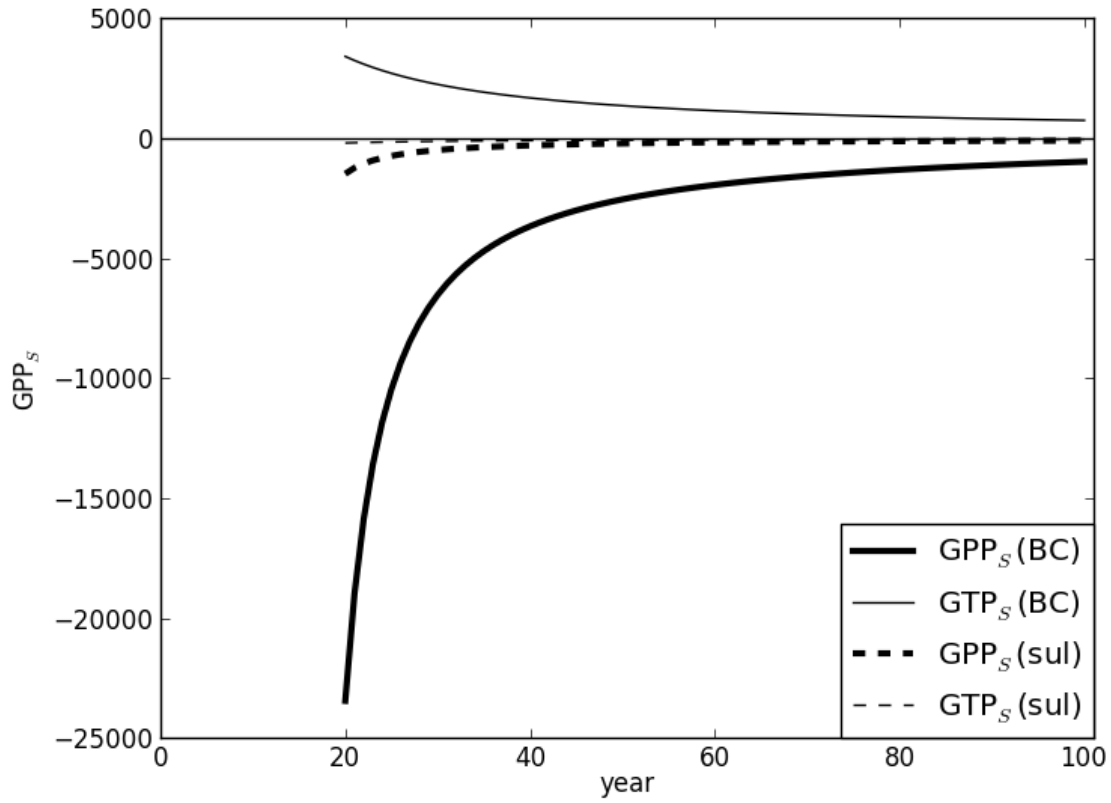


844

845 Figure 5: GPP_P (in bold) and GTP_P for 1 kg pulse emissions of BC and sulphate relative to a
846 1 kg pulse emission of CO₂.

847

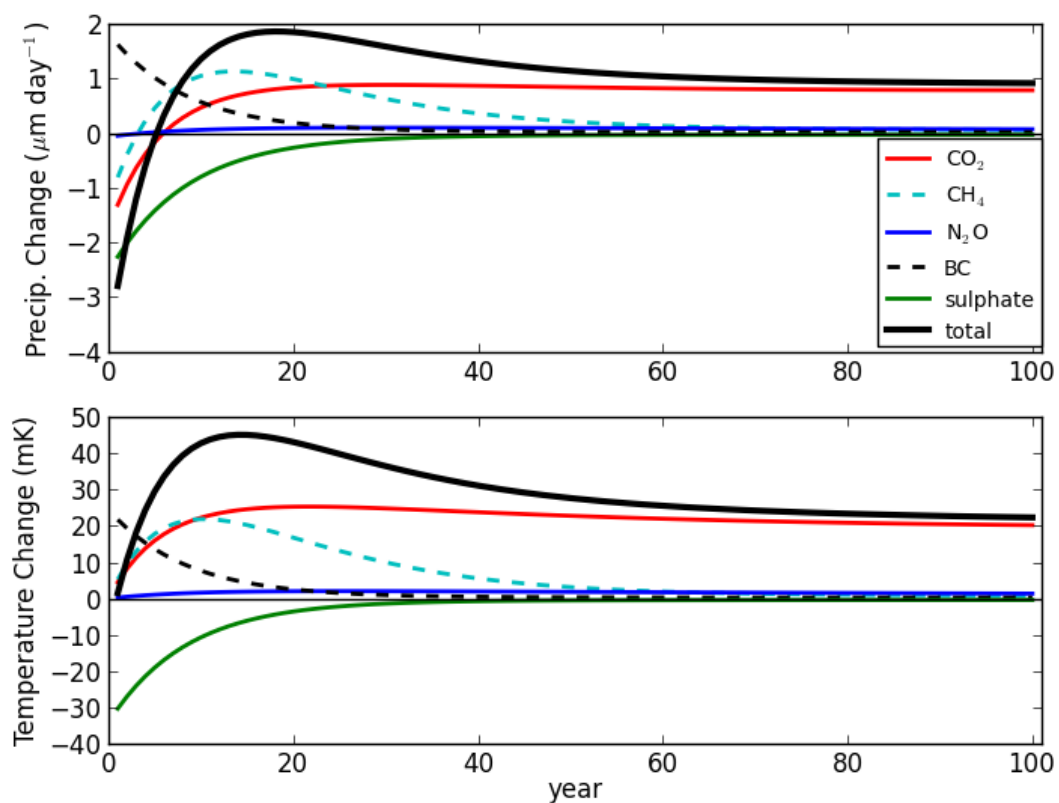
848



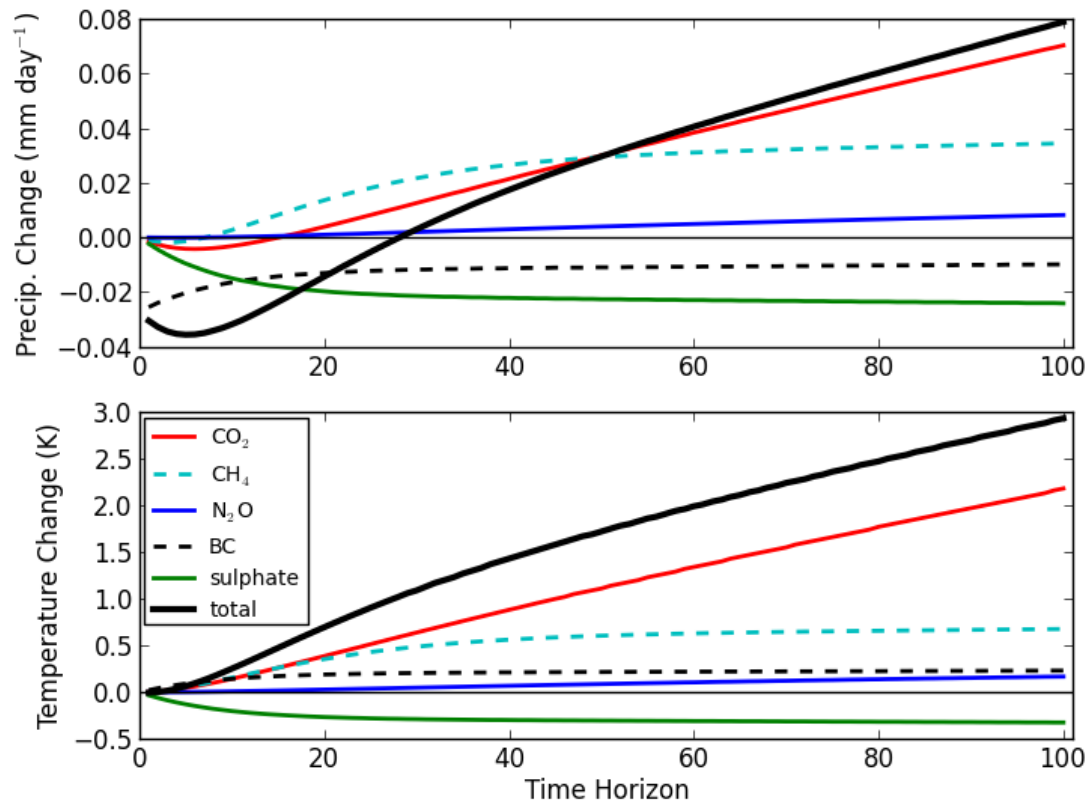
849

850 Figure 6. GPP_s (in bold) and GTP_s for 1 kg year⁻¹ sustained emissions of BC and sulphate

851 relative to a 1 kg year⁻¹ sustained emission of CO₂.

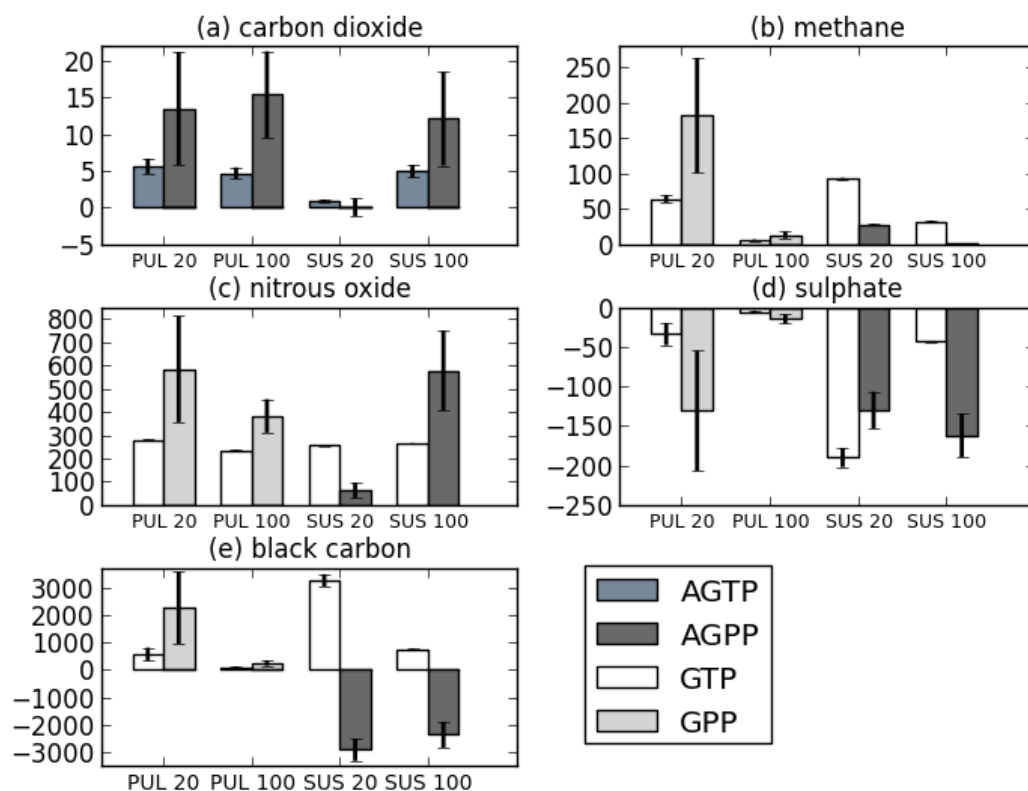


852
 853 Figure 7. Precipitation change, in $\mu\text{m day}^{-1}$ (top), and temperature change, in mK, (bottom) in
 854 the years after 2008, following a pulse emission in 2008, calculated using the AGPP_P and
 855 AGTP_P and using estimated emissions of the species in 2008.



856

857 Figure 8. Precipitation change, in mm day⁻¹ (top), and temperature change, in K, (bottom) in
 858 the years after 2008, assuming constant emissions at 2008 levels, calculated using the AGPP_S
 859 and AGTP_S and using estimated emissions of the species in 2008.



860

861 Figure 9: Mean and standard deviations of the AGTP, AGPP, GTP and GPP for both pulse
 862 (PUL) and sustained (SUS) emissions for time horizons of 20 and 100 years (which are
 863 chosen for illustrative purposes), using 18 different representations of the impulse-response
 864 function for temperature change. (a) AGTP and AGPP for carbon dioxide, for both pulse and
 865 sustained emissions, and then GTP_P, GPP_P, GTP_S and AGPP_S for (b) methane, (c) nitrous
 866 oxide, (d) sulphate and (e) black carbon. For CO₂ the units are 10⁻¹⁶ K kg⁻¹ for AGTP_P, 10⁻¹⁴
 867 K kg⁻¹ year for AGTP_S, 10⁻¹⁸ mm day⁻¹ kg⁻¹ for AGPP_P and 10⁻¹⁶ mm day⁻¹ kg⁻¹ year for
 868 AGPP_S. The AGPP_S for all other gases are in 10⁻¹⁵ mm day⁻¹ kg⁻¹ year.